AEROFOIL DESIGN FOR MAN POWERED AIRCRAFT

by Professor F X Wortmann, University of Stuttgart

Paper Presented at the Royal Aeronautical Society Symposium on "Man Powered Flight - The Way Ahead" held on 7 February 1977.

Aerofoil Design for Man Powered Aircraft

by

F.X.Wortmann

Universität Stuttgart

1. Design objectives for MPA aerofoils

Man powered aircraft are highly specialized machines not only from the structural point of view but also aerodynamically. They fly in a low Reynolds number range which is practically unexplored. On the other side, the requirements with respect to suitable aerofoils for the wing are much simpler than with sailplanes, since these machines are aimed to fly mostly between the best glide ratio and the stalling speed. For the usual high aspect ratio wings the aerofoils should develop a low drag minimum for c_L-values between 1.0 to 1.4 at Reynolds numbers from $3 \cdot 10^5$ to $7 \cdot 10^5$. These numbers depend only slightly on the specific design.

For the usual approach of splitting the total drag of the aircraft into a constant value c_{Do} and a lift dependent part the c_L-value for the maximum glide ratio becomes

$$c_{L\,opt}^2 = \pi\, c_{Do} \cdot A \qquad A = \text{Aspect ratio}$$

and for the minimum sinking speed

$$c_{L\,opt}^2 = 3\pi\, c_{Do}\, A$$

In order to have a reasonable margin to the stall the c_{Lmax} should be at least near 1.7 or 1.8. It is not so much the value of the c_{Lmax} but the stall behaviour which influences the flight safety. For this reason I would not recommend so-called maximum-lift aerofoils /1/.

Structural reasons ask for thick aerofoils. However, at these low Reynolds numbers aerofoil thickness has a much stronger influence on the drag than at higher Reynolds numbers, and their use should be restricted to the wingroot.

Since the necessary lift range is rather small the whole aerofoil problem can be reduced to the question: how can we attain low drag at these Reynolds numbers? I would like to simplify these matters even further and try to answer this question at first for symmetrical aerofoils. In a second step it is not too difficult to add a suitable camber and to look for an acceptable stall behaviour.

2. Drag of symmetrical aerofoils at low Reynolds numbers

Reliable drag measurements in the Reynolds number range of $3 - 7 \cdot 10^5$ are very rare. Therefore some exploratory tests were done in the laminar wind tunnel of the University of Stuttgart on some typical symmetrical aerofoils, which for two aerofoils go down to $Re = 3 \cdot 10^5$. In order to illustrate the allimportant transition control, two very different aerofoils have been selected and their velocity distribution at $\alpha = 0^\circ$ is given in Fig.1.

The first one, designated IS-30A/150, has a thickness of 15% and resembles in the front part a typical "laminar" aerofoil. Between 40 to 70% of the chord there exists a weak adverse pressure gradient called instability range /2/, which should destabilize the laminar boundary layer and provoke transition in front of the strong adverse pressure gradient. If this fails to work the laminar boundary layer will separate at the start of the strong pressure gradient at $x/c = .68$. The observed positions of the transition at several Reynolds numbers are indicated. It is somewhat surprising to see that the laminar boundary layer which downstream of $x/c = .4$ closely approaches separation needs a Reynolds number of three millions to become turbulent in front of the $x/c = .68$ station. For lower Reynolds numbers there develops a laminar separation bubble. The reattachment point seems to stop at $x/c = .76$.

The drag of this particular aerofoil at $\alpha = 0^\circ$ is shown in Fig.2 together with two other aerofoils. Below a Reynolds number of $1.2 \cdot 10^6$ the drag of the IS-30A/150 increases disproportionally. Obviously, the velocity distribution of this aero-

foil is despite the long instability range not very well adapted to the laminar boundary layer which develops for a Reynolds number below $1.2\ 10^6$.

In contrast to this example, Fig.1 shows also the very different velocity distribution of the FX 76-120. Now the velocity peak is near the nose and followed by a weak and long adverse pressure gradient which smoothly changes into a slightly increased pressure gradient near the trailing edge. The separation point for the potential velocity distribution is close to $x/c = .6$.

Despite the long adverse pressure gradient the transition is observed downstream of the inviscous separation point for Reynolds numbers at $Re = 10^6$, and all the more at lower Reynolds numbers. In Fig.2 the drag of this aerofoil, which is with 12% slightly thinner than the first one, is nearly constant between $0.7 < Re < 1.5\ 10^6$. A 10% thick version of the 76-120 was also measured and has a similar drag behaviour. The drag of $7.5\ 10^{-3}$ at $Re = 3 \cdot 10^5$ is remarkably low. The transition was observed at $x/c = .95$. The $c_L(\alpha)$ and drag polar are given in Fig.3.

3. Transition control

At higher Reynolds numbers the region of transition is usually so small that the term transition point is justified. At Reynolds numbers below one million the process of transition into a fully developed turbulent boundary layer takes more and more space and time and the type of transition control seems to get the overriding influence on the drag. Obviously, velocity distributions of the first aerofoil (IS-30A/150) offer no chance of low drag at $Re < 10^6$. This holds not only for $\alpha = 0^o$ but even more at larger angles of attack. Fig.4 compares the drag polars of these two aerofoils. Again the aerofoil 76-120 becomes the better one below $Re = 10^6$ at all angles of attack. In order to put these observations on a more general basis we may ask: do we have an empirical relationship which correlates the transition Reynolds number for non-separating laminar boundary layers?

Fig.5 gives such a relationship. re_ϑ is the Reynolds number of the boundary layer momentum thickness and $H_{32} = \delta^{**}/\vartheta$ the shape parameter (δ^{**} = energy thickness). Typical values of H_{32} are 1.572 for the flat plate and 1.515 for separation. The line "Instability" averages different results of the linear stability theory. Any combination of $re\ (H_{32})$ above this line may amplify small perturbations and eventually lead to transition. The broad band indicates many empirical observations in different wind tunnels. Obviously, the position of transition will depend on the type and size of perturbations in the whole unstable region between instability and transition. Due to the unknown input of perturbations in different wind tunnels, in free flight (high up or down in the shear layer of the natural wind) we cannot expect a very reliable relationship.

There are three lines given: the empirical relationships of Granville /3/ and v.Driest /4/ and simply a line of Δre_ϑ = const = 800. Finally, the transition measurements of Fig.1 and some others from our laminar wind tunnel are given with the shaded area. It can be seen that most of the criteria yield a too early transition for the unseparated laminar boundary layer. For a quiet atmosphere it may be that transition occurs even later.

Obviously, for the low Reynolds numbers of man powered flight we have to live with laminar separation bubbles, because only the separated boundary layer has the capability to become turbulent at a length scale less than the whole chord length. Such sort of transition control, however, has to be handled with care. Experimental evidence as in Fig.1 with the IS 30 aerofoil or other even more drastic examples /5/ indicates that a laminar separation bubble which extends into a strong adverse pressure gradient has a very detrimental influence on the turbulent boundary layer. Comparing Fig.1 and Fig.2 it can be seen that the bubble length of the IS-aerofoil is unchanged below Re = 1.5 10^6, however, the drag increases disproportionally. It seems to be far better to apply only weak pressure gradients as with the 76-120 in Fig.1 which alleviate

the reattachment process and the start of the turbulent wall boundary layer. At the same time this type of velocity distribution is not sensitive to changes in Reynolds numbers and angles of attack and may be a "practical" solution.

For the transition downstream of separation there seems not to exist any reliable empirical relationship. At least, three parameters are now involved: the momentum Reynolds number of the laminar boundary layer in the separation point, the level of preamplified perturbations at this point and finally the shape or thickness of the bubble, which seems to be correlated with the overall pressure gradient between separation and reattachment.

At this point it may be appropriate to mention shortly the structural problems to obtain smooth aerofoil surfaces with thin membranes. The slight changes of the aerofoil contour due to the double curvature of the skin does practically not disturb the flow over straight wings, however, a wedgelike nose or a kink in the chordwise contour is not tolerable. Therefore any type of construction should and could easily be tested with full scale models to ensure that laminar flow exists up to at least 70% of the chord on both sides of the model. The stethoscope is the cheap instrument to certify this fact.

4. Aerofoil design for the wing of man powered aircraft

On the basis of the foregoing considerations four aerofoils with a thickness ratio of 12, 14, 16 and 18% have been designed. The shape of these aerofoils and the 76-100 symmetrical aerofoil are given in Fig.6. Table 1 gives the coordinates. The thinner aerofoils are intended for the medium and outer wing sections. In this part of the wing the aileron effectiveness is important and a smaller thickness is in general favorable in this respect.

At the same time the 12 and 14% aerofoils have additional characteristics which should improve the stall behaviour. This feature is illustrated in Fig.7.

At high angles of attack the velocity distribution on the upper side near the x/c = .07 station has a short region where the steep adverse pressure gradient is reduced to avoid a thick laminar separation bubble and to favour the turbulent reattachment. The lower part of Fig.7 gives the curvature distribution, which also reflects this particular feature. It is the same type of boundary control as for low angles of attack, now applied at the nose to improve the high-lift case. It has been proven /5/ that this concept works even if the transition control cannot be perfect due to too low Reynolds numbers.

With an improved initial development of the turbulent boundary layer on the upper side we can expect a separation position near the x/c = .7 position, which will not change very much with increasing angles of attack. Only the downstream angle of the separation region, which acts like a negatively deflected fluid flap, will increase, which in turn holds the pressure distribution over the forward part of the aerofoil and hence the overall lift nearly constant. It is hoped that at least some of these sections will be tested up to the time the lecture will be given.

References

/1/ F.X.Wortmann, "The Quest for High Lift". AIAA Paper 74-1018, MIT - Cambridge, Sept.1974.

/2/ F.X.Wortmann, "Experimentelle Untersuchungen an neuen Laminarprofilen für Segelflugzeuge und Hubschrauber". Zeitschr.f.Flugwissenschaften 5(1957), S.228-234.

/3/ P.S.Granville, "The calculation of viscous drag of bodies of revolution". David Taylor Model Basin Rep.849(1953).

/4/ E.R.v.Driest, C.B.Blumer, "Boundary layer transition". AIAA J. 1963, Vol.I, pp.1303-1306.

/5/ F.X.Wortmann, "Design of airfoils with high lift at low and medium subsonic Mach numbers". AGARD CP-102 (1972), Lisbon.

NR	FX 76-100 X/T	FX 76-100 YO/T	FX 76-100 YU/T	FX 76-120 X/T	FX 76-120 YO/T	FX 76-120 YU/T
1	1.00000	.00000	.00000	1.00000	.00000	.00000
2	.99891	.00076	-.00076	.99891	.00000	.00000
3	.99571	.00100	-.00100	.99571	.00073	-.00073
4	.99034	.00155	-.00155	.99034	.00099	-.00099
5	.98291	.00240	-.00240	.98291	.00163	-.00163
6	.97344	.00346	-.00346	.97344	.00263	-.00263
7	.96192	.00465	-.00465	.96192	.00389	-.00389
8	.94848	.00609	-.00609	.94848	.00531	-.00531
9	.93299	.00773	-.00773	.93299	.00703	-.00703
10	.91571	.00959	-.00959	.91571	.00900	-.00900
11	.89644	.01161	-.01161	.89644	.01123	-.01123
12	.87590	.01385	-.01385	.87590	.01366	-.01366
13	.85350	.01614	-.01614	.85350	.01635	-.01635
14	.82970	.01862	-.01862	.82970	.01911	-.01911
15	.80435	.02105	-.02105	.80435	.02211	-.02211
16	.77773	.02359	-.02359	.77773	.02502	-.02502
17	.74995	.02604	-.02604	.74995	.02809	-.02809
18	.72115	.02858	-.02858	.72115	.03104	-.03104
19	.69133	.03096	-.03096	.69133	.03411	-.03411
20	.66074	.03340	-.03340	.66074	.03698	-.03698
21	.62938	.03562	-.03562	.62938	.03992	-.03992
22	.59750	.03789	-.03789	.59750	.04260	-.04260
23	.56525	.03991	-.03991	.56525	.04534	-.04534
24	.53274	.04201	-.04201	.53274	.04777	-.04777
25	.49997	.04371	-.04371	.49997	.05032	-.05032
26	.46733	.04540	-.04540	.46733	.05237	-.05237
27	.43469	.04665	-.04665	.43469	.05439	-.05439
28	.40243	.04802	-.04802	.40243	.05590	-.05590
29	.37056	.04892	-.04892	.37056	.05755	-.05755
30	.33933	.04973	-.04973	.33933	.05865	-.05865
31	.30861	.05012	-.05012	.30861	.05962	-.05962
32	.27891	.05035	-.05035	.27891	.06009	-.06009
33	.24998	.05019	-.05019	.24998	.06038	-.06038
34	.22221	.04978	-.04978	.22221	.06019	-.06019
35	.19558	.04894	-.04894	.19558	.05970	-.05970
36	.17037	.04777	-.04777	.17037	.05869	-.05869
37	.14643	.04615	-.04615	.14643	.05730	-.05730
38	.12403	.04408	-.04408	.12403	.05535	-.05535
39	.10330	.04149	-.04149	.10330	.05287	-.05287
40	.08422	.03845	-.03845	.08422	.04976	-.04976
41	.06694	.03500	-.03500	.06694	.04612	-.04612
42	.05158	.03130	-.03130	.05158	.04198	-.04198
43	.03802	.02728	-.02728	.03802	.03753	-.03753
44	.02650	.02310	-.02310	.02650	.03272	-.03272
45	.01702	.01871	-.01871	.01702	.02770	-.02770
46	.00960	.01419	-.01419	.00960	.02243	-.02243
47	.00422	.00941	-.00941	.00422	.01701	-.01701
48	.00102	.00457	-.00457	.00102	.01128	-.01128
49	.00000	.00000	.00000	.00000	.00548	-.00548

FX 76 MP 120

NR	X/T	YO/T	YU/T
1	1.00000	.00000	.00000
2	.99891	.00151	-.00047
3	.99571	.00311	.00058
4	.99034	.00542	.00220
5	.98291	.00836	.00426
6	.97344	.01184	.00661
7	.96192	.01579	.00904
8	.94848	.02032	.01153
9	.93299	.02537	.01393
10	.91571	.03102	.01622
11	.89644	.03720	.01827
12	.87590	.04396	.02009
13	.85350	.05122	.02153
14	.82970	.05898	.02265
15	.80435	.06720	.02337
16	.77773	.07581	.02379
17	.74995	.08462	.02387
18	.72115	.09335	.02377
19	.69133	.10161	.02351
20	.66074	.10912	.02320
21	.62938	.11573	.02276
22	.59750	.12143	.02223
23	.56525	.12610	.02152
24	.53274	.12979	.02067
25	.49997	.13252	.01961
26	.46733	.13438	.01838
27	.43469	.13531	.01694
28	.40243	.13538	.01533
29	.37056	.13453	.01350
30	.33933	.13282	.01149
31	.30861	.13023	.00927
32	.27891	.12683	.00693
33	.24998	.12257	.00444
34	.22221	.11753	.00191
35	.19558	.11173	-.00067
36	.17037	.10526	-.00323
37	.14643	.09815	-.00572
38	.12403	.09059	-.00804
39	.10330	.08254	-.01013
40	.08422	.07411	-.01188
41	.06694	.06516	-.01323
42	.05158	.05590	-.01416
43	.03802	.04645	-.01446
44	.02650	.03737	-.01406
45	.01702	.02867	-.01269
46	.00960	.02073	-.01048
47	.00422	.01324	-.00737
48	.00102	.00679	-.00386
49	.00000	.00000	.00000

FX 76 MP 140

X/T	YO/T	YU/T
1.00000	.00000	.00000
.99891	.00145	-.00056
.99571	.00293	.00032
.99034	.00509	.00171
.98291	.00787	.00349
.97344	.01118	.00549
.96192	.01496	.00755
.94848	.01936	.00959
.93299	.02433	.01147
.91571	.02995	.01319
.89644	.03617	.01461
.87590	.04303	.01572
.85350	.05048	.01639
.82970	.05851	.01668
.80435	.06708	.01651
.77773	.07613	.01599
.74995	.08541	.01510
.72115	.09466	.01404
.69133	.10341	.01287
.66074	.11139	.01171
.62938	.11842	.01051
.59750	.12451	.00933
.56525	.12952	.00806
.53274	.13352	.00675
.49997	.13652	.00532
.46733	.13862	.00381
.43469	.13977	.00218
.40243	.14003	.00048
.37056	.13935	-.00136
.33933	.13779	-.00329
.30861	.13531	-.00534
.27891	.13200	-.00743
.24998	.12779	-.00958
.22221	.12277	-.01169
.19558	.11695	-.01376
.17037	.11043	-.01573
.14643	.10324	-.01755
.12403	.09557	-.01916
.10330	.08734	-.02043
.08422	.07869	-.02131
.06694	.06946	-.02171
.05158	.05986	-.02163
.03802	.04998	-.02085
.02650	.04044	-.01936
.01702	.03121	-.01688
.00960	.02273	-.01359
.00422	.01459	-.00938
.00102	.00750	-.00489
.00000	.00000	.00000

	FX-76-MP 160			FX-76-MP 180		
NR	X/T	YO/T	YU/T	X/T	YO/T	YU/T
1	1.00000	.00000	.00000	1.00000	.00000	.00000
2	.99891	.00126	.00045	.99891	.00113	.00045
3	.99571	.00264	.00066	.99571	.00264	.00046
4	.99034	.00493	.00145	.99034	.00461	.00099
5	.98291	.00762	.00312	.98291	.00713	.00242
6	.97344	.01090	.00458	.97344	.01027	.00354
7	.96192	.01462	.00663	.96192	.01381	.00526
8	.94848	.01904	.00809	.94848	.01814	.00626
9	.93299	.02392	.00992	.93299	.02292	.00764
10	.91571	.02958	.01085	.91571	.02859	.00800
11	.89644	.03567	.01202	.89644	.03469	.00859
12	.87590	.04257	.01210	.87590	.04175	.00796
13	.85350	.04984	.01225	.85350	.04919	.00740
14	.82970	.05790	.01116	.82970	.05757	.00546
15	.80435	.06626	.01012	.80435	.06627	.00358
16	.77773	.07531	.00787	.77773	.07580	.00037
17	.74995	.08442	.00575	.74995	.08539	-.00269
18	.72115	.09364	.00276	.72115	.09519	-.00668
19	.69133	.10221	.00029	.69133	.10427	-.01005
20	.66074	.11007	-.00262	.66074	.11265	-.01383
21	.62938	.11686	-.00482	.62938	.11987	-.01678
22	.59750	.12285	-.00742	.59750	.12630	-.02007
23	.56525	.12768	-.00932	.56525	.13147	-.02251
24	.53274	.13172	-.01175	.53274	.13587	-.02545
25	.49997	.13464	-.01350	.49997	.13905	-.02755
26	.46733	.13698	-.01589	.46733	.14170	-.03027
27	.43469	.13827	-.01761	.43469	.14320	-.03219
28	.40243	.13892	-.01995	.40243	.14410	-.03468
29	.37056	.13850	-.02164	.37056	.14385	-.03639
30	.33933	.13751	-.02396	.33933	.14305	-.03870
31	.30861	.13544	-.02557	.30861	.14109	-.04016
32	.27891	.13282	-.02779	.27891	.13862	-.04221
33	.24998	.12910	-.02919	.24998	.13494	-.04328
34	.22221	.12486	-.03111	.22221	.13077	-.04486
35	.19558	.11955	-.03214	.19558	.12542	-.04540
36	.17037	.11375	-.03362	.17037	.11961	-.04635
37	.14643	.10687	-.03407	.14643	.11261	-.04614
38	.12403	.09954	-.03483	.12403	.10515	-.04619
39	.10330	.09127	-.03444	.10330	.09664	-.04495
40	.08422	.08273	-.03410	.08422	.08786	-.04374
41	.06694	.07347	-.03249	.06694	.07823	-.04113
42	.05158	.06412	-.03099	.05158	.06851	-.03863
43	.03802	.05415	-.02819	.03802	.05805	-.03472
44	.02650	.04442	-.02544	.02650	.04783	-.03088
45	.01702	.03439	-.02124	.01702	.03716	-.02551
46	.00960	.02498	-.01697	.00960	.02713	-.02014
47	.00422	.01589	-.01129	.00422	.01729	-.01333
48	.00102	.00796	-.00567	.00102	.00866	-.00669
49	.00000	.00000	.00000	.00000	.00000	.00000

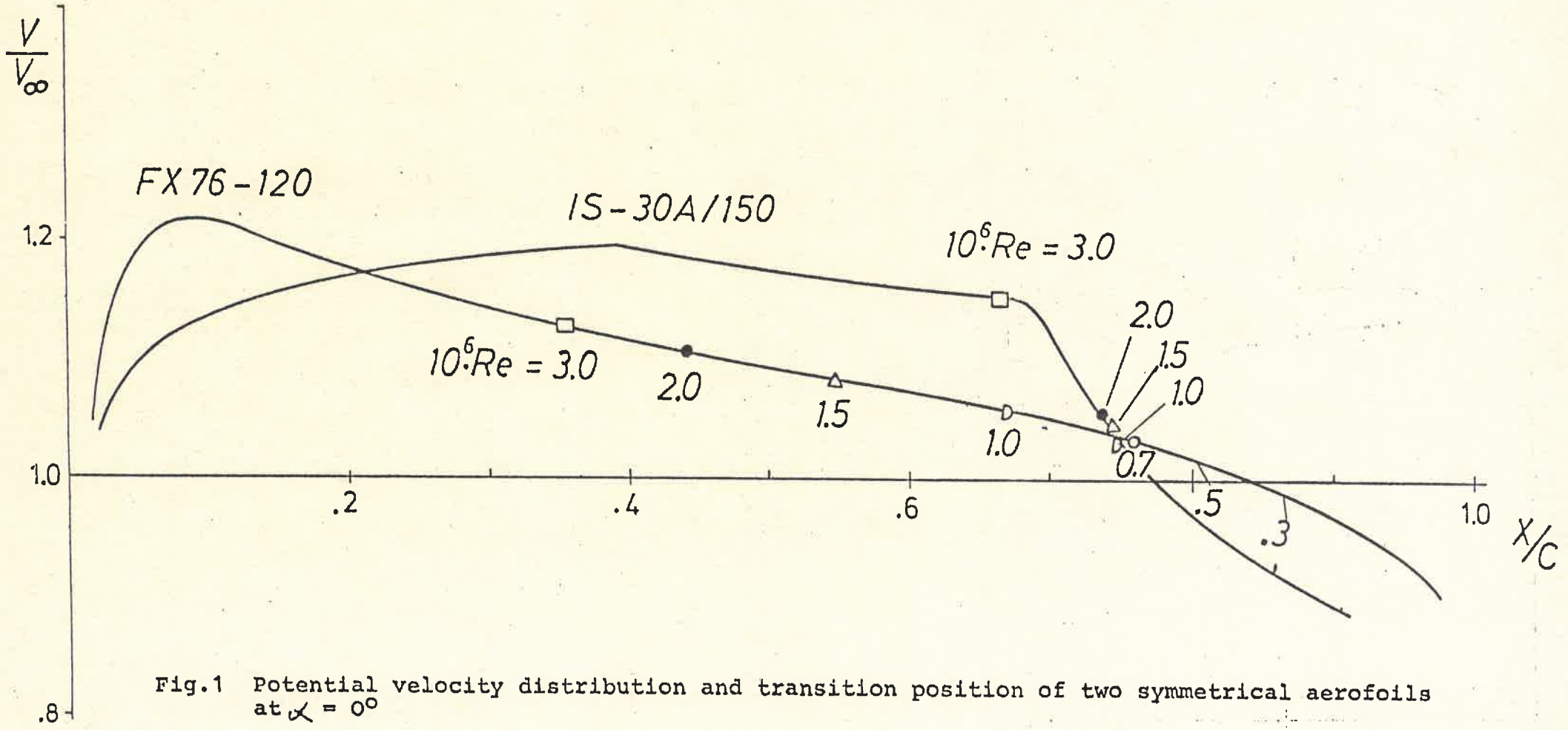

Fig.1 Potential velocity distribution and transition position of two symmetrical aerofoils at $\alpha = 0^{\circ}$

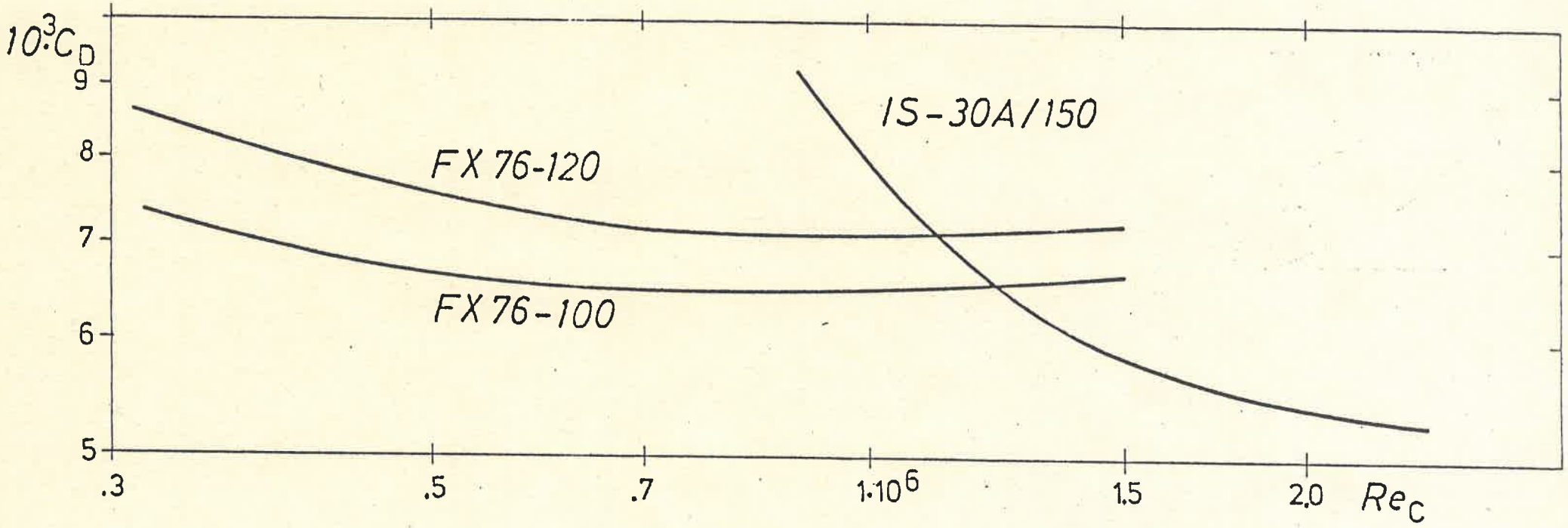

Fig.2 Drag values of three symmetrical aerofoils with 15, 12 and 10% thickness ratio and $\alpha = 0^o$ at Reynolds numbers between $3 \cdot 10^5$ to $2 \cdot 10^6$

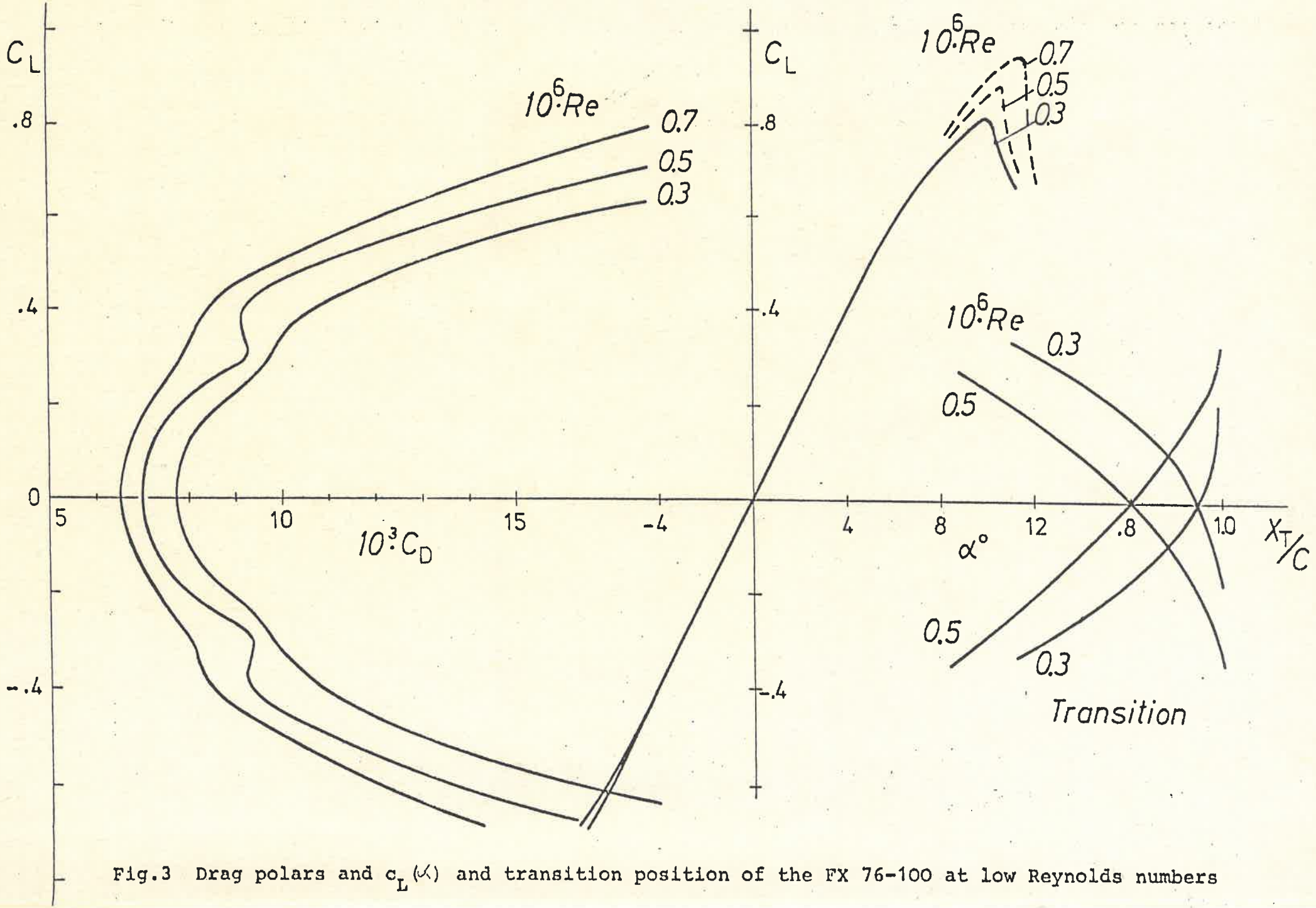

Fig.3 Drag polars and $c_L(\alpha)$ and transition position of the FX 76-100 at low Reynolds numbers

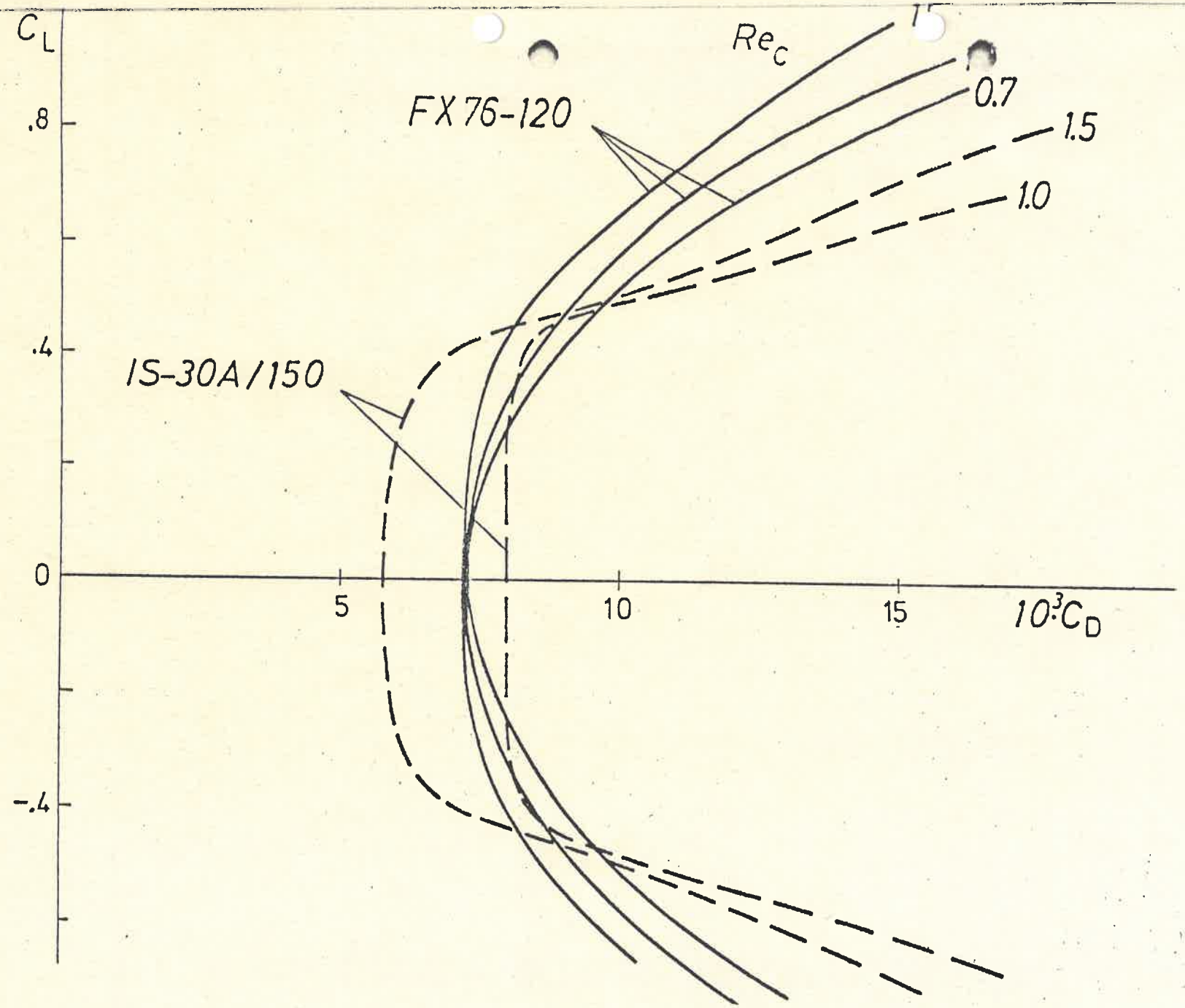

Fig.4 Drag polars of the IS-30A/150 and the FX 76-120 at Reynolds numbers near one million

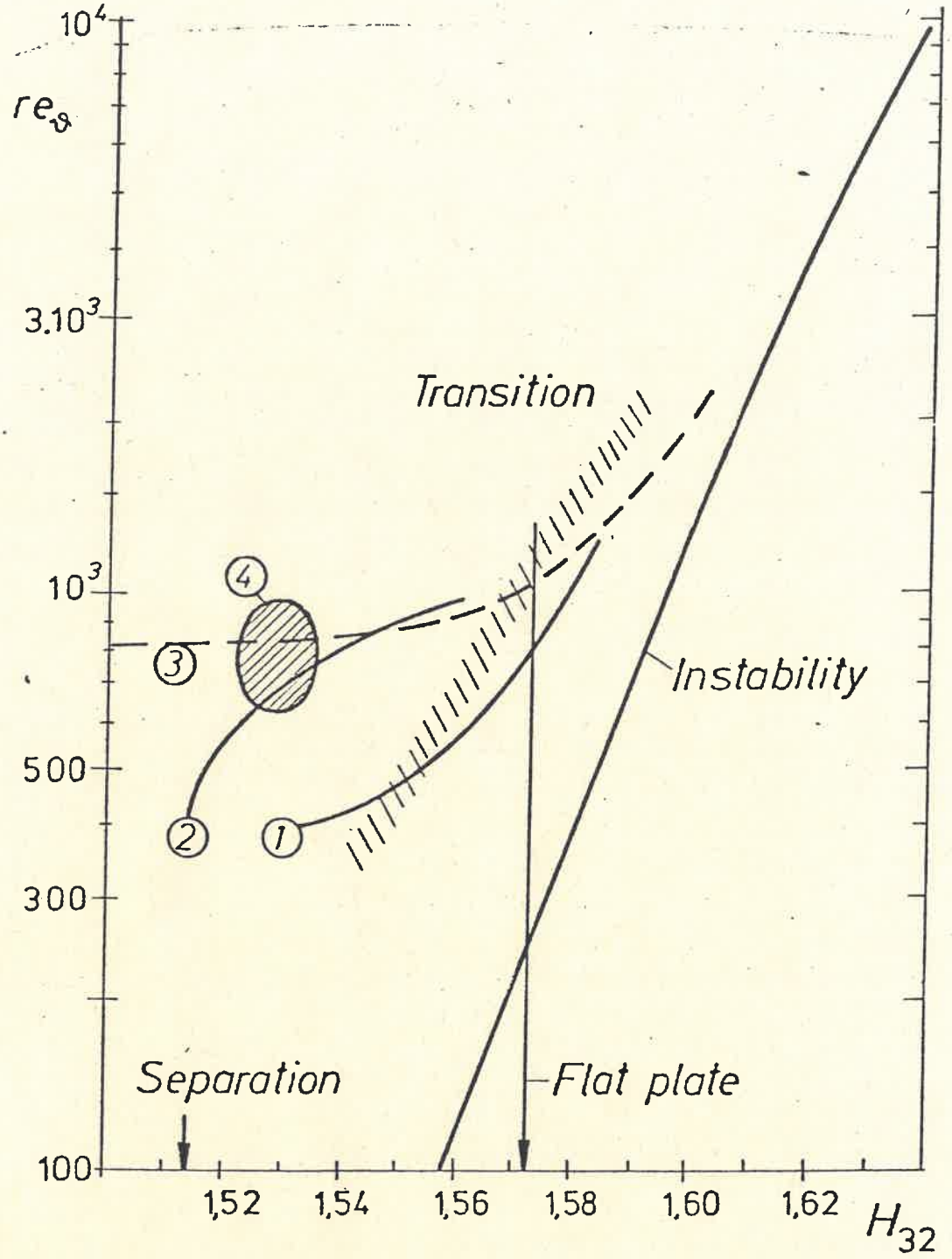

Fig.5 Momentum thickness Reynolds number of instability and transition as function of the shape parameter H_{32}

1 Granville
2 v.Driest
3 $\Delta re_\vartheta = 800$

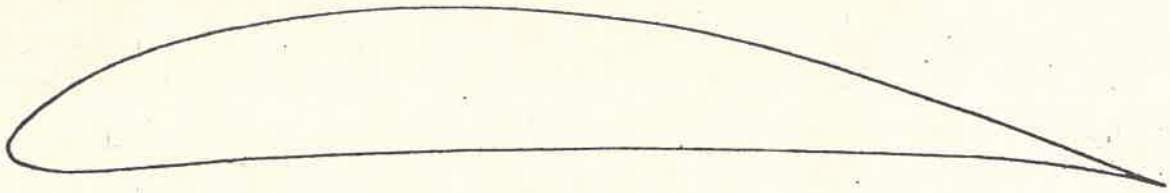

FX 76 - MP 120

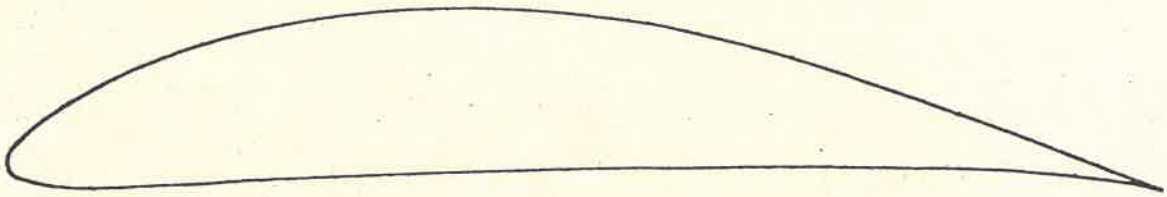

FX 76 - MP 140

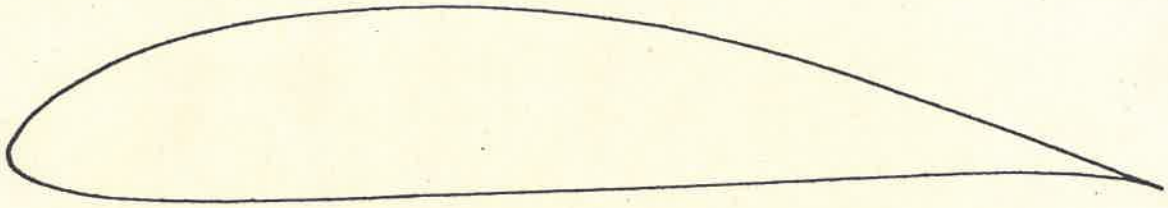

FX 76 - MP 160

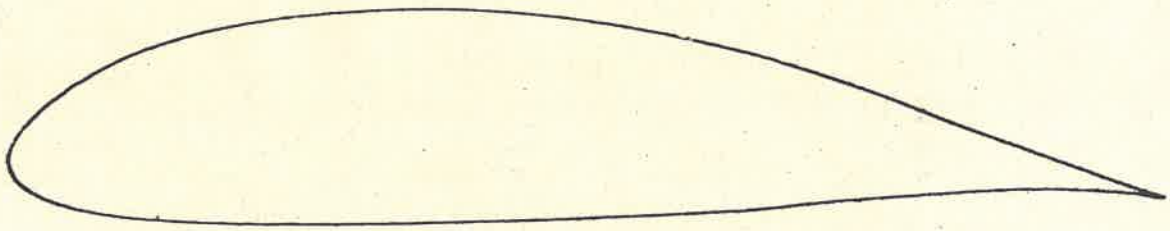

FX 76 - MP 180

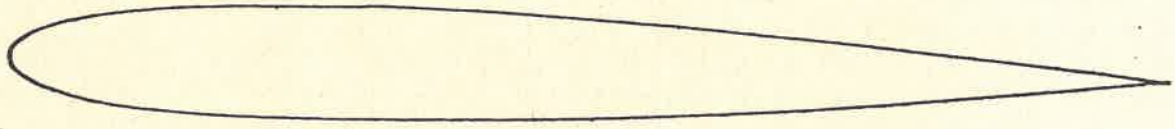

FX 76 - MP 100

Fig.6 Shape of some aerofoils designed for low Reynolds numbers

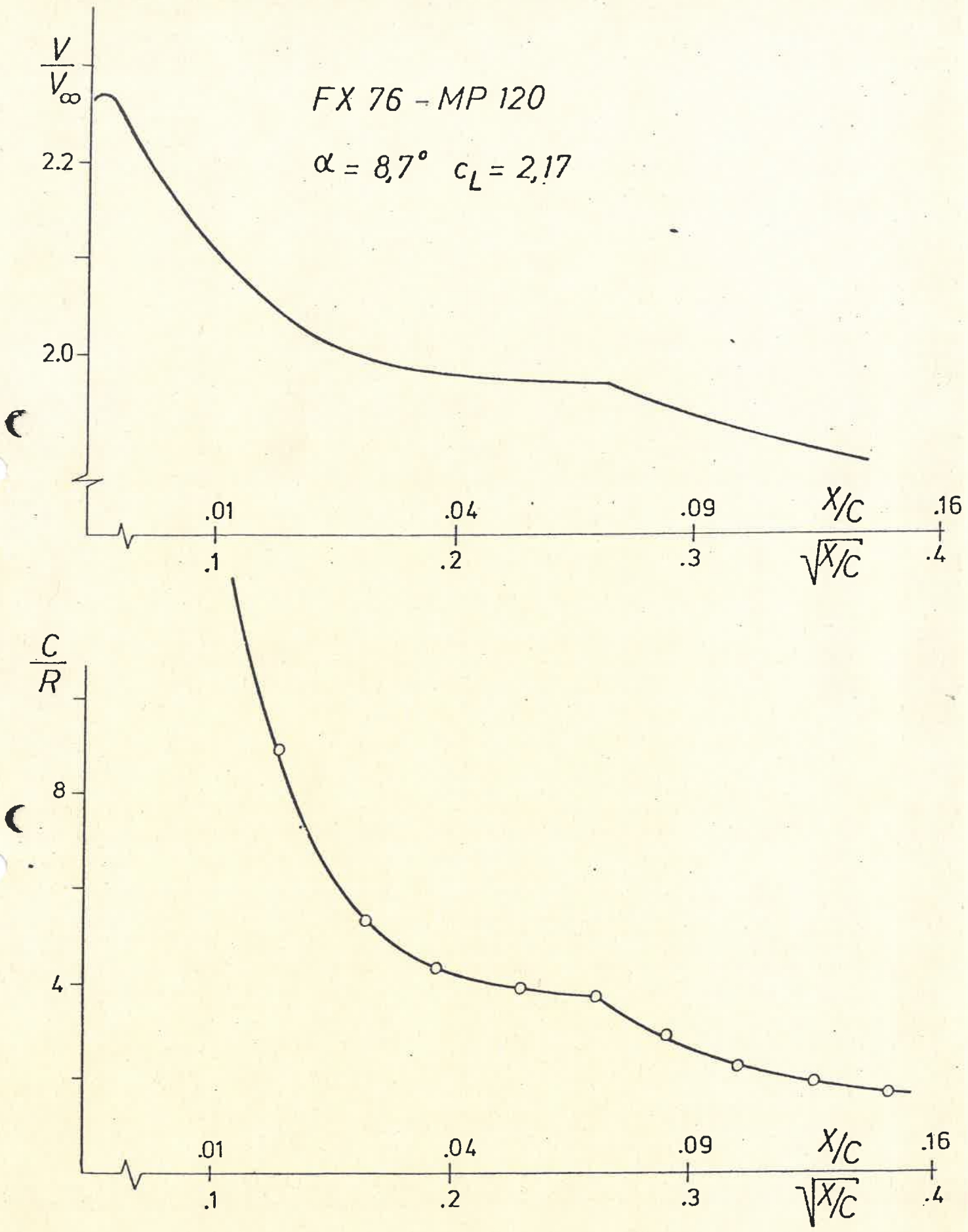

Fig.7 Velocity and curvature distribution of the FX 76-MP 120 near the nose